

Perturbations in a scalar field model with virtues of Λ CDM

Srijita Sinha* and Narayan Banerjee†

IISER Kolkata, Mohanpur Campus, Mohanpur, Nadia 741246, India

Abstract

In the era of precision cosmology, the cosmological constant Λ gives quite an accurate description of the evolution of the Universe, but it is still plagued with the fine-tuning problem and the cosmic coincidence problem. In this work, we investigate the perturbations in a scalar field model that drives the recent acceleration in a similar fashion that the cosmological constant does and has the dark energy (DE) density comparable to the dark matter (DM) energy density at the recent epoch starting from arbitrary initial conditions. The perturbations show that this model, though it keeps the virtues of a Λ CDM model, has a distinctive qualitative feature, particularly it reduces the amplitude of the matter power spectrum on a scale of $8h^{-1}$ Mpc, σ_8 at the present epoch.

PACS: 98.70.Vc, 04.25.Nx

Keywords: Cosmological perturbation theory, Dark energy theory, Power spectrum

1 Introduction

The recent cosmological observations using various independent observational data like the Type Ia Supernovae (SNe Ia) measurements [1–4], cosmic microwave background (CMB) [5–7], Particle Data Group [8], large scale structure (LSS) [9–12] show that the Universe is expanding with an acceleration for the past several Giga years. An exotic component called ‘dark energy’ (DE), in the Universe, can help overcome the attractive nature of gravity and make matter move away from each other at a faster rate. To drive the acceleration of the Universe, the pressure (p) of the DE must be sufficiently negative, making its ratio with the energy density (ρ) at least less than $-\frac{1}{3}$ ($p/\rho = w < -1/3$). A non-zero cosmological constant, Λ , is undoubtedly the preferred one [7, 13–17]. A scalar field with a potential, introduced by Peebles & Ratra [18] and Ratra & Peebles [19], is also a popular choice. A lot of work followed from there for various purpose. Some examples can be found in [20–29]. Other well-known options include Holographic Dark Energy [30–32], Chaplygin gas [33–35], phantom field [36–38], quintom model [39, 40] (where w evolve to mimic the phantom fluid) among many others. There are excellent reviews [41–44] that summarise the merits and problems of these candidates.

Over the last decade, the availability of high precision data from various surveys has suggested that $w = -1.03 \pm 0.03$ within the 95% confidence level [7], consistent with a cosmological constant. One is tempted to conclude that the cosmological constant as dark energy with cold dark matter (Λ CDM) is by far the most suitable model that describes the evolution of the Universe at the present epoch. But the Λ CDM model is plagued with problems like the fine-tuning problem [41] and the coincidence problem [45, 46]. The fine-tuning problem is that the initial conditions are needed to be set to an exact value so that the cosmological constant term dominates at the current epoch. The coincidence problem is related to the question why the energy densities of dark matter and dark energy are of the same order of magnitude at the present epoch. These problems in the Λ CDM model has forced us to look for other candidates that can drive the acceleration. A scalar field rolling down a slowly varying potential not only gives rise to acceleration but also alleviates the cosmological coincidence problem. Such a scalar field, dubbed as ‘quintessence’, has been studied extensively in the literature [18, 19, 47–66].

The ‘tracking’ model was first introduced by Ratra & Peebles [19] and Peebles & Ratra [18]. The idea was to resolve the fine-tuning problem, long before the discovery of the present accelerated expansion of the Universe. Some ‘scaling’ models, which alleviates the fine-tuning problem, were also discussed in [47–49, 63], which do not, however, drive the present acceleration. Zlatev *et al.* [53] and Steinhardt *et al.* [54] later utilised a modified version to incorporate the accelerated expansion. These ‘tracking’ models can resolve the fine-tuning problem and coincidence problem but cannot give rise to the acceleration with $w = -1$. The values of w that can be obtained are $w = -0.6$ [61], $w = -0.8$ [51], $w \approx -0.82$ [56], $w < -0.8$ [53, 57] to mention a few. Thus, none of the Λ CDM model and the quintessence models appear to be a complete solution, they are rather complementary to each other. One should therefore look for a model that will have

* ✉ ss13ip012@iiserkol.ac.in

† ✉ narayan@iiserkol.ac.in

the virtues of both the Λ CDM and a quintessence but will be devoid of the flaws. A ‘tracking’ quintessence model with an inverse power law potential, however, was shown to be consistent with observational data sets [67–70]. The inverse power law potential with a dynamical dark energy gives $w = -1.03 \pm 0.07$ within the 68.27% confidence limit [69], in agreement with the recent observations. However, the present model is different from that discussed in [51, 53, 56, 57, 61, 67–71] and yields $w = -1$ at the present epoch independent of the model parameters.

To construct a model without the problem of fixing the initial conditions, the ‘scaling’ potential or the ‘tracking’ potential is a natural choice. However, the scaling solution does not drive an acceleration, whereas the best-known tracking potentials cannot give the observationally preferred value of $w \simeq -1$. In the present work, we introduce a scalar field model with a potential such that it will have an accelerated expansion with an equation of state at the present epoch similar to that given by Λ CDM and the current dark energy density comparable to that of dark matter independent of the initial conditions. We engineer the model such that the scalar field ϕ is subdominant as a tracking dark energy at early times and start dominating as a cosmological constant in the recent past driving the acceleration. The presence of a scalar field from early times will have its imprints on the growth of perturbations and hence on the large scale structures of the Universe. The scalar field will evolve through the history of the Universe, and unlike Λ CDM, will have fluctuations similar to the other matter components. These fluctuations will affect the formation of structures [72] and can also cluster on their own [73, 74]. Thus, structure formation will help break the degeneracy between the Λ CDM model and our scalar field model (ϕ CDM). This work aims to investigate the perturbation in such a dark energy model and look for the distinguishing features from the standard Λ CDM model. The present work is not an attempt to constrain the model parameters with the observational datasets but rather to bring out the characteristic features of the model by solving the perturbation equations. It must be mentioned that the motivation of this work is not to unify inflation and dark energy and we will consider the evolution of the ϕ CDM long after the completion of inflation.

The paper is organised as follows. We start with a brief discussion on the scalar field model and introduce the potential in Sect. 2. In Sect. 3, starting from the relevant perturbation equations we discuss the evolution of the density contrasts along with the CMB temperature fluctuation, matter power spectrum, linear growth rate and $f\sigma_8$. Finally, in Sect. 4, we summarise and discuss the conclusive results that we arrive at.

2 The scalar field model

We consider a homogeneous and isotropic Universe with spatially flat constant time hypersurface, described by the well-known Friedmann-Lemaître-Robertson-Walker (FLRW) metric as,

$$ds^2 = a^2(\tau)(-d\tau^2 + \delta_{ij}dx^i dx^j), \quad (1)$$

where $a(\tau)$ is the scale factor and the conformal time τ is related to the cosmic time t as $a^2 d\tau^2 = dt^2$. The Universe is filled with non-interacting fluids, namely photons (γ), neutrinos (ν), baryons (b), cold dark matter (c) and a scalar field (ϕ) with a potential $V(\phi)$ acting as dark energy. The Friedmann equations are given as

$$3\mathcal{H}^2 = -a^2 \kappa \sum_i \rho_i, \quad (2)$$

$$\mathcal{H}^2 + 2\mathcal{H}' = a^2 \kappa \sum_i p_i, \quad (3)$$

where $\kappa = 8\pi G_N$ (G_N being the Newtonian Gravitational constant), $\mathcal{H}(\tau) = \frac{a'}{a}$ is the conformal Hubble parameter and prime ($'$) denotes the derivative with respect to the conformal time. The energy density and pressure of each component are respectively ρ_i and p_i , where $i = \gamma, \nu, b, c, \phi$. The equation of state (EoS) parameter is given as $w_i = \frac{p_i}{\rho_i}$. For the photons and neutrinos, $w_\gamma = w_\nu = 1/3$, for baryons and CDM, $w_b = w_c = 0$. For the scalar field, $\rho_\phi = \frac{1}{2a^2} \phi'^2 + V(\phi)$ and $p_\phi = \frac{1}{2a^2} \phi'^2 - V(\phi)$ and the EoS parameter is given by

$$w_\phi = \frac{p_\phi}{\rho_\phi} = \frac{\frac{1}{2a^2} \phi'^2 - V(\phi)}{\frac{1}{2a^2} \phi'^2 + V(\phi)} = 1 - \frac{2V(\phi)}{\rho_\phi}. \quad (4)$$

The Klein-Gordon equation can be obtained as a consequence of the Bianchi identities as

$$\phi'' + 2\mathcal{H}\phi' + a^2 \frac{dV}{d\phi} = 0. \quad (5)$$

It is clear from the expression (4) that w_ϕ has an evolution and ranges between $-1 \leq w_\phi \leq 1$ for a real scalar field and a positive definite $V(\phi)$. When the kinetic energy ($E_K = \frac{\phi'^2}{2a^2}$) is dominant with a negligible potential energy ($E_P = V(\phi)$), the scalar field behaves as a stiff fluid with $w_\phi = 1$, and when E_P dominates with a negligible E_K , it gives rise to a cosmological constant with $w_\phi = -1$. Thus, the behaviour of the scalar field and hence the evolution of the Universe

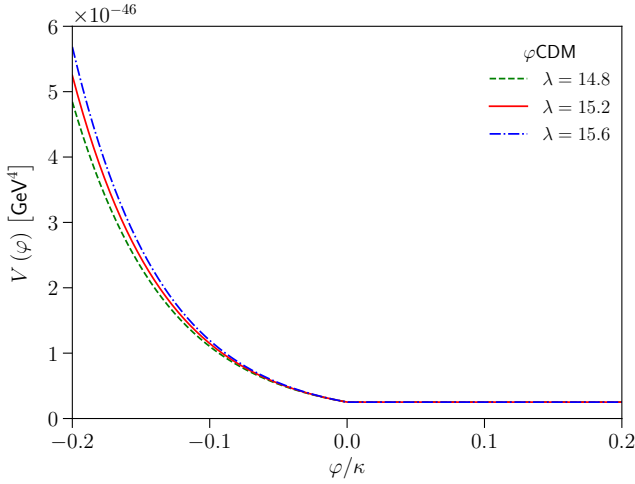


Figure 1: Plot of the potential $V(\varphi)$ in units of GeV^4 against φ/κ with $V_0 = 2.510 \times 10^{-47} \text{ GeV}^4$ and $\lambda = 14.8$ (dashed line), $\lambda = 15.2$ (solid line) and $\lambda = 15.6$ (dashed-dot line). Changing V_0 will change $\Omega_{\varphi 0}$.

depends on the form of the potential. For the recent accelerated expansion of the Universe, the scalar field at late time should roll sufficiently slowly along the potential such that $E_K \ll E_P$.

We construct the potential such that the scalar field behaves as a quintessence field in the past and a cosmological constant in the present. We consider the potential as the sum of an exponential potential and a constant potential, shown in Fig. (1). The potential is written as,

$$V(\varphi) = V_0 e^{-\lambda \kappa \varphi} \Theta(-\varphi) + V_0 \Theta(\varphi), \quad (6)$$

where V_0 is a constant and $\Theta(\varphi)$ is the Heaviside theta defined as

$$\Theta(\varphi) = \begin{cases} 0 & \varphi < 0, \\ 1 & \varphi \geq 0. \end{cases} \quad (7)$$

The potential given in Eqn. (6) is continuous. In the exponential part, the scalar field tracks the evolution of the dominant background fluid with $w_\varphi = w_D$ and $\Omega_\varphi = 3(1+w_D)/\lambda^2$ with the condition $\lambda^2 > 3(1+w_D)$, w_D being the EoS parameter of the background fluid and Ω_φ is the energy density parameter defined as $\frac{\rho_\varphi}{3H^2/\kappa}$. Here, H is the Hubble parameter defined with respect to the cosmic time t . This attractor solution is called the ‘scaling solution’, introduced by Ratra & Peebles in [19] (see also [47–49]). The scalar field then leaves the scaling regime and enters the constant potential regime. The constant part of the potential arrests the fall of the scalar field and it starts to slow-roll and eventually dominate the energy density of the Universe as the cosmological constant. This drives an accelerated expansion at a late time with $w_\varphi = -1$.

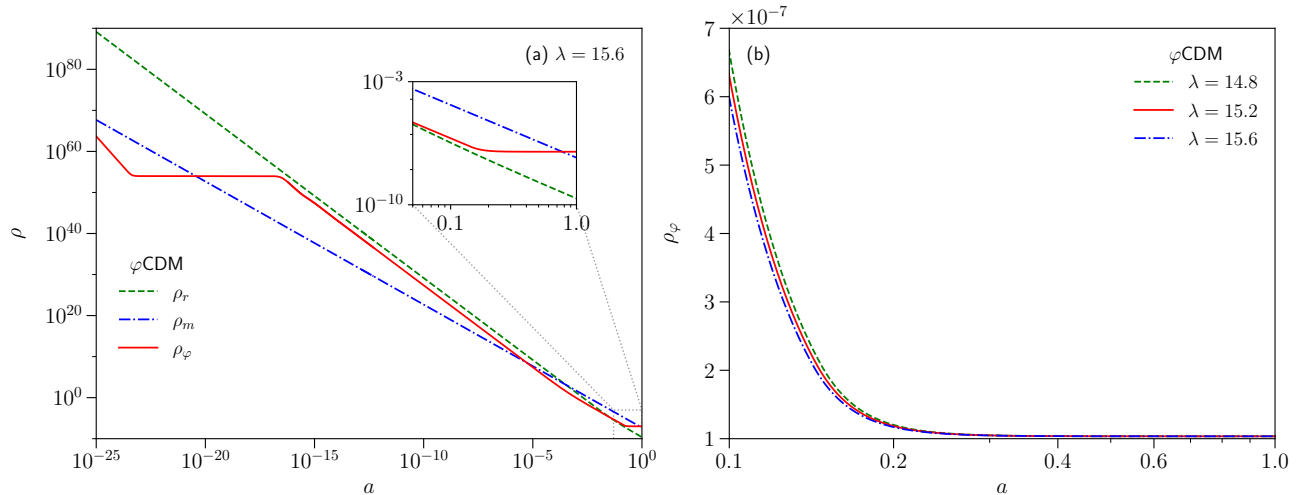


Figure 2: (a) Plot of energy density ρ against scale factor a in logarithmic scale where the role of dark energy is played by a scalar field (φ) in presence of photons (γ), neutrinos (ν), baryons (b), cold dark matter (c). For simplicity, only radiation ($r \equiv \gamma + \nu$) and matter ($m \equiv b + c$) are shown along with φ , labelling the model as φCDM . The late time evolution of ρ is enlarged in the inset. Only $\lambda = 15.6$ is considered here. (b) Plot of ρ_φ against scale factor a shows that the evolution of ρ_φ at late time is same for different values of the model parameter λ for a fixed value of V_0 .

Fig. (2a) shows the variation of the energy density of radiation, ρ_r ($r \equiv \gamma + \nu$), matter, ρ_m ($m \equiv b + c$) and scalar field, ρ_φ , with the scale factor a in logarithmic scale. Before reaching the tracking mode, the scalar field evolves through

different regimes as shown in Fig. (2a). We integrate the Klein-Gordon equation (5) numerically, using the potential (6), starting from $a = 10^{-25}$ and consider that the initial ρ_ϕ is smaller than ρ_r and ρ_m at that epoch. As ϕ rolls down the potential, $E_K \gg E_P$ suppressing $\frac{dV}{d\phi}$ relative to the first two terms in Eqn. (5). E_K redshifts as a^{-6} while E_P remains constant and ρ_ϕ is dominated by E_K . This kinetic-dominated regime is followed by the potential-dominated regime, where ϕ rolls down very slowly making ϕ'' inconsequential. In this regime ρ_ϕ is determined by $V(\phi)$ and becomes flat as ϕ hardly evolves. When the dominant background, ρ_r in this case, reaches the flat attractor value, they start evolving together. Thereafter, ρ_ϕ tracks ρ_r and subsequently ρ_m , depending on which dominates the background as discussed by Ratra & Peebles [19]. For a single component background along with the scalar field, such as pure radiation and pure matter, similar results can be obtained analytically as well [19, 54, 75]. Later, when the constant potential V_0 takes over, the scalar field energy density, ρ_ϕ behaves like the cosmological constant. It should be noted that this transition is instantaneous as it is implemented by a step function. Figure (2b) confirms that the cosmological constant like behaviour is ensured for any value of the parameter λ for a given value of V_0 .

The advantages of this potential (6) are that at late time $w_\phi = -1$, irrespective of the model parameters, λ and V_0 , or initial conditions and that the fraction of dark energy density present today, $\Omega_{\phi 0}$ depends on the height of the slow-roll region, V_0 . It deserves mention that V_0 is not a free parameter but is fixed by the other model parameters like the $\Omega_b h^2$, $\Omega_c h^2$, H_0 , such that $\Omega_{\phi 0}$ matches the observed value of Ω_Λ (~ 0.6847) [7]. The Θ function switches off the effect of the exponential potential in the constant potential part so that the scalar field is dominated completely by the E_P after leaving the scaling region. It deserves mention that the value of ϕ for the transition from exponential to constant potential is a free parameter. The effect in the evolution of the scalar field due to the change in the transition value can be seen from Fig. (3), where we consider three examples. When the transition point is shifted from zero to ϕ_0 , the exponential part of the potential, Eqn. (6) changes as $V_0 e^{-\lambda\kappa(\phi-\phi_0)}$ to accommodate for the continuity of $V(\phi)$. The change in the steepness of the exponential potential changes the evolution of the scalar field before it behaves as a tracking field. Once it starts to track the dominant background components, its evolution remains unaffected by the change in the transition point, ϕ_0 . So without loss of much of generality, we define our potential with $\phi_0 = 0$.

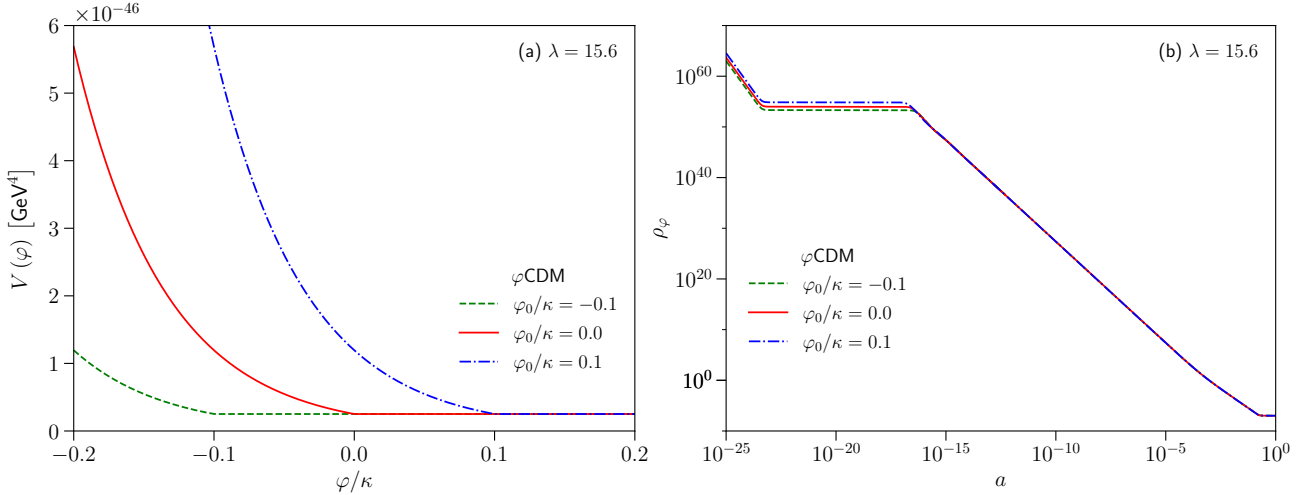


Figure 3: (a) Plot of the potential $V(\phi)$ in units of GeV^4 against ϕ/κ with $V_0 = 2.510 \times 10^{-47} \text{ GeV}^4$, $\lambda = 15.6$ and transition at $\phi_0/\kappa = -0.1$ (dashed line), $\phi_0/\kappa = 0.0$ (solid line) and $\phi_0/\kappa = 0.1$ (dashed-dot line). Changing V_0 will change $\Omega_{\phi 0}$. (b) Plot of ρ_ϕ against scale factor a shows that the evolution of ρ_ϕ is different only at early times for different values of transition point ϕ_0 for fixed values of V_0 and λ .

The constraint on the parameter λ comes from Big Bang Nucleosynthesis (BBN) condition [48–50],

$$\Omega_\phi(a \sim 10^{-10}) \lesssim 0.09. \quad (8)$$

It should be noted that in all the subsequent discussion, the scale factor, a , is scaled so that its present value, $a_0 = 1$. Considering $V_0 = 2.510 \times 10^{-47} \text{ GeV}^4$ and $\lambda = 15.6$ with the parameter values listed in Table 1 gives $\Omega_\phi(a \sim 10^{-10}) = 0.01642$ and $\Omega_\phi(a = 1) = 0.6840$. The parameter values listed in Table 1, are taken from the latest data release in 2018 of the *Planck* collaboration [7] (*Planck* 2018, henceforth) and are based on the fiducial spatially flat ΛCDM model. For our calculation we have considered $\phi_i = -\frac{8.99}{\kappa}$ at $a_i = 10^{-25}$. It turns out that $\phi = 0$ at $a = 0.14237$ (for the values of V_0 and λ chosen), where the potential changes its role from a scaling potential to effectively a cosmological constant. The dimensionless density parameter, Ω_i is given by $\frac{\rho_i}{3H^2/\kappa}$ where the suffix i stands for the i -th component. The dimensionless Hubble parameter at the present epoch is defined as $h = \frac{H_0}{100 \text{ km s}^{-1} \text{ Mpc}^{-1}}$. Figure (2) is obtained by solving the Klein-Gordon Eqn. (5) numerically with the potential (6) using these parameter values. For the study of detailed dynamics of the scalar field during tracking region we refer to [19, 47–49, 54, 75].

Table 1: Values of background parameters from the *Planck* 2018 collaboration.

Parameter	Value
$\Omega_b h^2$	0.0223828
$\Omega_c h^2$	0.1201075
H_0 [km s ⁻¹ Mpc ⁻¹]	67.32117

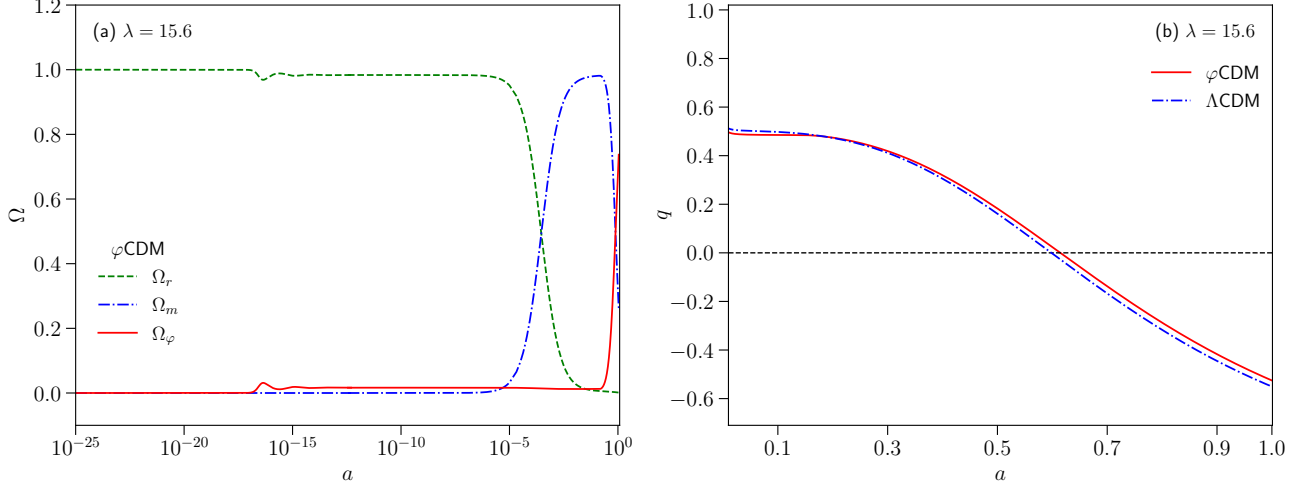


Figure 4: (a) Plot of density parameter Ω against scale factor a in logarithmic scale. For simplicity, only radiation ($r \equiv \gamma + \nu$) and matter ($m \equiv b + c$) are shown along with ϕ . (b) Plot of deceleration parameter q against scale factor a for ϕ CDM (solid line) and Λ CDM (dashed-dot line). Only $\lambda = 15.6$ is considered here.

The evolution of the energy density parameters, Ω ($\equiv \Omega_i$) of radiation ($r \equiv \gamma + \nu$), matter ($m \equiv b + c$) and scalar field (ϕ) with the scale factor a , in logarithmic scale, are shown in Fig. (4a) and that of the deceleration parameter $q = -\left(\frac{a a''}{a'^2} - 1\right)$ with a in Fig. (4b) for $\lambda = 15.6$. Figure (4) shows that the evolution dynamics of the Universe is different from the Λ CDM model even though $w_\phi = -1$ at the present epoch. The two models are qualitatively very similar, but not really overlapping. For the scalar field model, henceforth called ϕ CDM, the accelerated expansion starts at a little higher value of a compared to the Λ CDM model.

3 The perturbations

The scalar field model given by Eqn. (6) can have fluctuations and thereby affect the evolution of perturbations of other components. The scalar perturbation equations in synchronous gauge are considered in the present work and the differential equations are solved using the suitably modified version of the publicly available Boltzmann code CAMB¹ [76]. To study the dependence of the fluctuations on the model parameters, we used different values of λ keeping V_0 constant (varying V_0 will change $\Omega_{\phi 0}$).

3.1 Effect on density perturbation

The scalar perturbation of the FLRW metric takes the form [77]

$$ds^2 = a^2(\tau) \left\{ -(1 + 2\phi)d\tau^2 + 2\partial_i B d\tau dx^i + [(1 - 2\psi)\delta_{ij} + 2\partial_i \partial_j E] dx^i dx^j \right\}, \quad (9)$$

where ϕ, ψ, B, E are gauge-dependent functions of both space and time. In synchronous gauge, $\phi = B = 0$, $\psi = \eta$ and $k^2 E = -h/2 - 3\eta$, where η and h are the synchronous gauge fields defined in the Fourier space and k is the wavenumber [78]. The perturbation equations in the matter sector in the Fourier space are

$$\delta'_i + k v_i + \frac{h'}{2} = 0, \quad (10)$$

$$v'_i + \mathcal{H} v_i = 0, \quad (11)$$

¹<https://camb.info>

where $\delta_i = \delta\rho_i/\rho_i$ is the density contrast and v_i is the peculiar velocity of i -th ($i = b, c$) fluid. Assuming there is no momentum transfer in CDM frame, v_c is set to zero. For the details of this set of equations, we refer to the works [78–81]. The perturbation $\delta\varphi$ in the scalar field has the equation of motion [82]

$$\delta\varphi'' + 2\mathcal{H}\delta\varphi' + k^2\delta\varphi + a^2\frac{d^2V}{d\varphi^2}\delta\varphi + \frac{1}{2}\varphi'h' = 0, \quad (12)$$

in the Fourier space with wavenumber k . The perturbation in energy density $\delta\rho_\varphi$ and pressure δp_φ are given as

$$\delta\rho_\varphi = -\delta T_{0(\varphi)}^0 = \frac{\varphi'\delta\varphi'}{a^2} + \delta\varphi\frac{dV}{d\varphi}, \quad (13)$$

$$\delta T_{0(\varphi)}^j = -\frac{ik_j\varphi'\delta\varphi}{a^2}, \quad i \equiv \sqrt{-1} \quad (14)$$

$$\delta p_\varphi\delta_j^i = \delta T_{j(\varphi)}^i = \left(\frac{\varphi'\delta\varphi'}{a^2} - \delta\varphi\frac{dV}{d\varphi}\right)\delta_j^i, \quad (15)$$

when expanded in the Fourier space. Here $\delta T_{\nu(\varphi)}^\mu$ is the perturbed stress-energy tensor of the scalar field.

For an adiabatically expanding Universe, the square of sound speed is $c_{s,\varphi}^2 = p'_\varphi/\rho'_\varphi$. Using the Klein-Gordon Eqn. (5), the square of adiabatic sound speed [75, 83] for the scalar field reads as

$$c_{s,\varphi}^2 = -\frac{1}{3} - \frac{2\varphi''}{3\mathcal{H}\varphi'} = 1 + \frac{2a^2}{3\mathcal{H}\varphi'}\frac{dV}{d\varphi}. \quad (16)$$

In order to solve the perturbation Eqn. (12), the second derivative of the potential is written in terms of the square of sound speed, $c_{s,\varphi}^2$ as

$$\frac{d^2V}{d\varphi^2} = \frac{3}{2}\frac{\mathcal{H}^2}{a^2}\left[\frac{c_{s,\varphi}^{2'}}{\mathcal{H}} - \frac{1}{2}(c_{s,\varphi}^2 - 1)(3c_{s,\varphi}^2 + 5) + \frac{\mathcal{H}'}{\mathcal{H}}(c_{s,\varphi}^2 - 1)\right]. \quad (17)$$

The square of sound speed, $c_{s,\varphi}^2$ is constant in the different phases of evolution, e.g. in the scaling regime $c_{s,\varphi}^2 = w_\varphi = w_D$ and in the slow-roll regime $c_{s,\varphi}^2 = 1$. We shall henceforth take it to be described by Eqn. (16) but neglect its derivative, $c_{s,\varphi}^{2'}$ [75] in Eqn. (17). The perturbation Eqns. (10) and (11) are solved along with Eqns. (12), (13) and (14) with adiabatic initial conditions and $k = [1.0, 0.1, 0.01] h \text{ Mpc}^{-1}$ using CAMB.

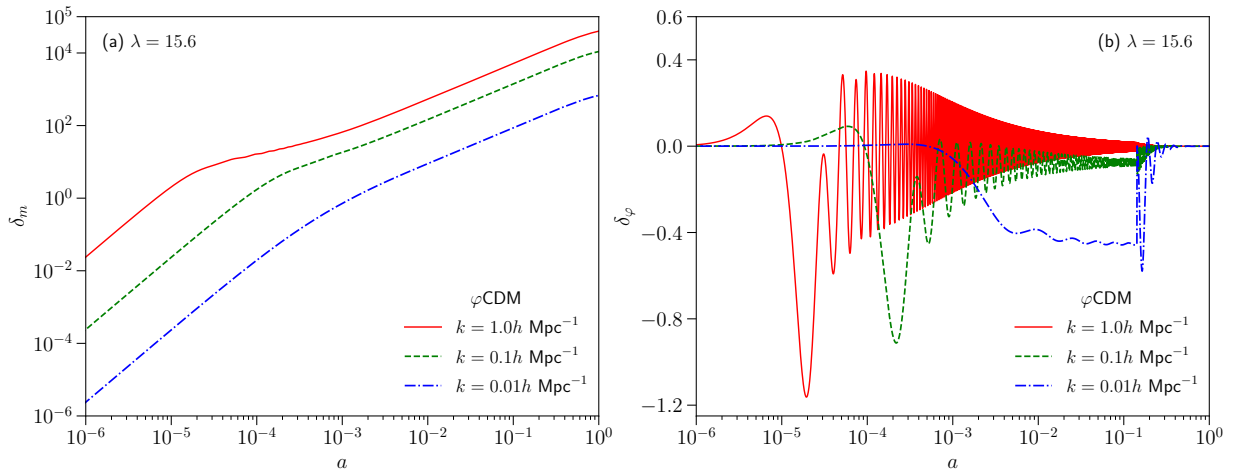


Figure 5: (a) Plot of the matter density contrast δ_m against a . Both the axes are in logarithmic scale. (b) Plot of scalar field density contrast δ_φ against a . In (b), only a in logarithmic scale. The solid line represents $k = 1.0 h \text{ Mpc}^{-1}$, dashed line represents $k = 0.1 h \text{ Mpc}^{-1}$ and dashed-dot line represents $k = 0.01 h \text{ Mpc}^{-1}$ with $\lambda = 15.6$.

Figure (5a) shows the variation of the density contrast, $\delta_m = \delta\rho_m/\rho_m$ for the cold dark matter (c) together with the baryonic matter (b) and Fig. (5b) shows the variation of the density contrast $\delta_\varphi = \delta\rho_\varphi/\rho_\varphi$ of the scalar field against a in logarithmic scale for $k = [1.0, 0.1, 0.01] h \text{ Mpc}^{-1}$. In the matter dominated era, the modes of δ_m grow in a very similar fashion. The modes of δ_φ oscillate rapidly with decreasing amplitude after entering the horizon. Figure (6) shows the evolution of the matter density contrast δ_m , for φCDM and ΛCDM . For a better comparison, δ_m for both the models have been scaled by $\delta_{m0} = \delta_m(a = 1)$ of ΛCDM . It can be seen that there is a difference in the growth of δ_m in the two models (φCDM and ΛCDM). To distinguish the effect of the parameter, λ , of the present potential with the ΛCDM model, we have shown the fractional matter density contrast, $\frac{\Delta\delta_m}{\delta_{m,\Lambda\text{CDM}}} = \left(1 - \frac{\delta_{m,\varphi\text{CDM}}}{\delta_{m,\Lambda\text{CDM}}}\right)$ in the lower panel of Fig. (6). It is clearly seen that, δ_m for $\lambda = 15.2$ takes a slightly smaller value compared to that of δ_m for $\lambda = 15.6$. Thus, the growth of matter density fluctuation decreases with decrease in the parameter, λ .

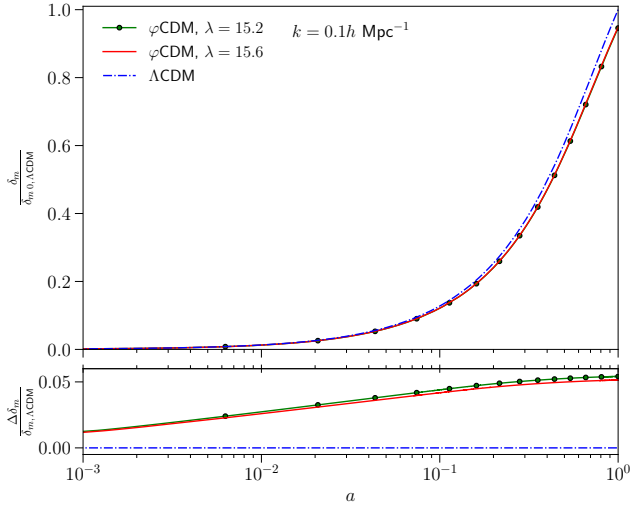


Figure 6: **Upper Panel** : Plot of the matter density contrast $\frac{\delta_m}{\delta_{m0,\Lambda\text{CDM}}}$ against a in logarithmic scale for ϕCDM with $\lambda = 15.2$ (solid line with solid circles) and $\lambda = 15.6$ (solid line) and ΛCDM (dashed-dot line) for $k = 0.1 h \text{ Mpc}^{-1}$. The difference in the growth of δ_m for ϕCDM and ΛCDM is prominent in the recent past, so the plot starts from $a = 10^{-3}$. **Lower Panel** : Plot of the fractional growth rate relative to the ΛCDM model. The fractional growth rate is defined as $\frac{\Delta\delta_m}{\delta_{m,\Lambda\text{CDM}}} = \left(1 - \frac{\delta_{m,\phi\text{CDM}}}{\delta_{m,\Lambda\text{CDM}}}\right)$.

3.2 Effect on CMB temperature, matter power spectra and $f\sigma_8$

For more insight into the effect of the scalar field ϕ on different physical quantities, we look at the CMB temperature spectrum, matter power spectrum and $f\sigma_8$. The CMB temperature power spectrum is given as

$$C_\ell^{TT} = \frac{2}{k} \int k^2 dk P_\zeta(k) \Delta_{T\ell}^2(k), \quad (18)$$

where $P_\zeta(k)$ is the primordial power spectrum, $\Delta_{T\ell}(k)$ is the temperature transfer function, ℓ is the multipole index and T stands for temperature. For the detail calculation of the CMB spectrum we refer to [84, 85]. The matter power spectrum is given as

$$P(k, a) = A_s k^{n_s} T^2(k) D^2(a), \quad (19)$$

where A_s is the normalising constant, n_s is the spectral index, $T(k)$ is the matter transfer function and $D(a) = \frac{\delta_m(a)}{\delta_m(a=1)}$ is the normalised density contrast. For the detailed method of calculation we refer to the monograph by Dodelson [86]. The C_ℓ^{TT} and $P(k, a)$ are computed numerically using CAMB. The values $A_s = 2.100549 \times 10^{-9}$ and $n_s = 0.9660499$ are taken from the *Planck* 2018 data [7], and hence, depend on the fiducial ΛCDM model. Figure (7a) shows that the CMB temperature power spectra, C_ℓ^{TT} , are almost independent of the values of the model parameter, λ . For clarity of the plots only two values of λ are given. The presence of the scalar field ϕ decreases the matter content of the Universe slightly during matter domination making the amplitude of first two peaks of the CMB spectra marginally higher than that in the ΛCDM model. The scalar field also lowers the low- ℓ CMB spectrum through the integrated Sachs-Wolfe (ISW) effect. These features are clear from the lower panel of Fig. (7a), which shows the fractional change ($= \Delta C_\ell^{TT} / C_{\ell,\Lambda\text{CDM}}^{TT}$) in C_ℓ^{TT} of the ϕCDM models relative to the ΛCDM model; a smaller λ produces slightly lower low- ℓ modes. A lesser amount of matter leads to a marginally lower matter power spectrum at small scales (Fig. (7b)), which is clear from the positive fractional change in matter power spectrum, $\Delta P / P_{\Lambda\text{CDM}}$, relative to the ΛCDM model (lower panel). Both these figures are for the present epoch.

To differentiate the ϕCDM and ΛCDM decisively, we have studied the linear growth rate,

$$f(a) = \frac{d \ln \delta_m}{d \ln a} = \frac{a}{\delta_m(a)} \frac{d \delta_m}{d a}. \quad (20)$$

Observationally the growth rate is measured using the perturbation of the galaxy density δ_g , which is related to the matter density perturbations δ_m as $\delta_g = b \delta_m$, where $b \in [1, 3]$ is the bias parameter. The estimate of the growth rate f is sensitive to the bias parameter, and thus not very reliable. A more dependable observational quantity is the product $f(a)\sigma_8(a)$ [87], where $\sigma_8(a)$ is the root-mean-square (rms) fluctuations of the linear density field within the sphere of radius $R = 8h^{-1} \text{ Mpc}$. The rms mass fluctuation can be written as $\sigma_8(a) = \sigma_8(1) \frac{\delta_m(a)}{\delta_m(1)}$, where $\sigma_8(1)$ is the value at $a = 1$ (Table 2), calculated by integrating the matter power spectrum over all the values of the wavenumber k using CAMB. Thus, the combination becomes

$$f\sigma_8(a) \equiv f(a)\sigma_8(a) = \sigma_8(1) \frac{a}{\delta_m(1)} \frac{d \delta_m}{d a}. \quad (21)$$

Since $f\sigma_8$ measurements provide a tighter constraint on the cosmological parameters, it will give a better insight into the growth of the density perturbations. We have studied the variation of f and $f\sigma_8$ with redshift z for three different values of λ . Redshift z is related to the scale factor a as $z = \left(\frac{a_0}{a} - 1\right)$, a_0 being the present value. The linear growth rate f and $f\sigma_8$ are independent of the wavenumber k for low redshift. As the $f\sigma_8$ analysis is valid for $z \in [0, 2]$, the redshift from $z = 0$ to $z = 2$ are considered here.

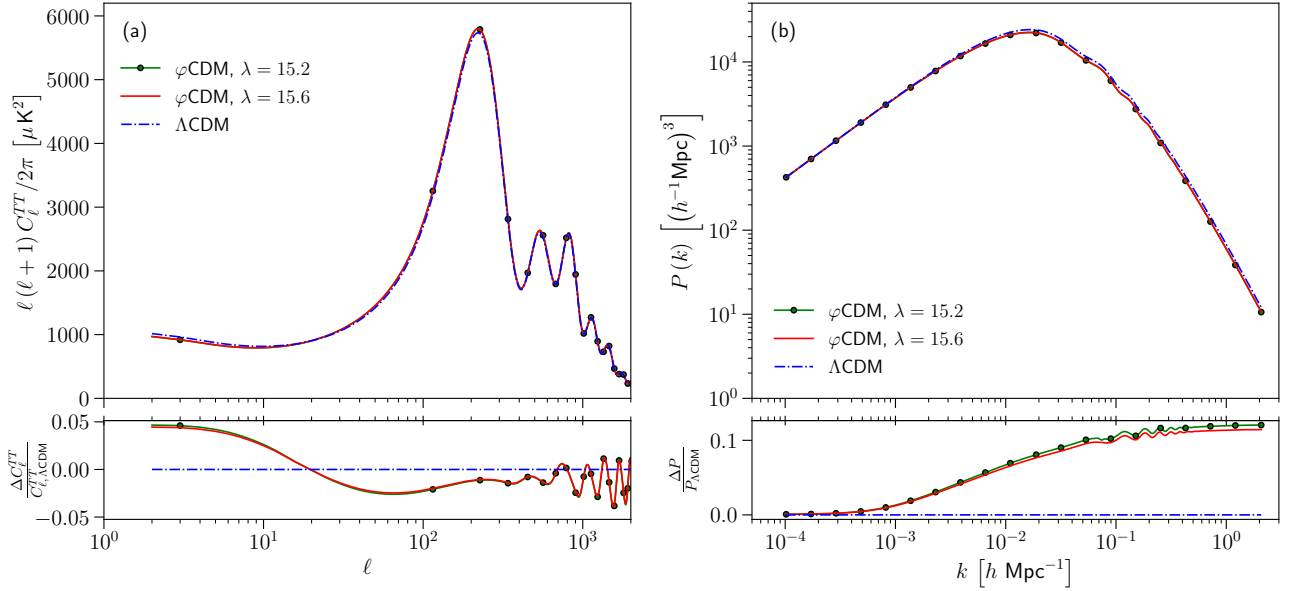


Figure 7: **Upper Panel** : (a) Plot of CMB temperature power spectrum in units of μK^2 with the multipole index ℓ in logarithmic scale. (b) Plot of matter power spectrum $P(k)$ in units of $(h^{-1}\text{Mpc})^3$ with wavenumber k in units of $h\text{Mpc}^{-1}$. Both the axes are in logarithmic scales in (b). **Lower Panel** : Plot of fractional change in the temperature spectrum, $\frac{\Delta C_\ell^{TT}}{C_{\ell, \Lambda\text{CDM}}^{TT}} = \left(1 - \frac{C_{\ell, \phi\text{CDM}}^{TT}}{C_{\ell, \Lambda\text{CDM}}^{TT}}\right)$ and the fractional change in matter power spectrum, $\frac{\Delta P}{P_{\Lambda\text{CDM}}} = \left(1 - \frac{P_{\phi\text{CDM}}}{P_{\Lambda\text{CDM}}}\right)$ For both panels, the solid line with solid circles represents ϕ CDM with $\lambda = 15.2$ and solid line represents ϕ CDM with $\lambda = 15.6$ while the dashed-dot line is for Λ CDM at $a = 1$.

Table 2: Values of σ_8 at $a = 1$ for the ϕ CDM and Λ CDM models.

Model	λ	σ_8
ϕ CDM	14.8	0.7638
	15.2	0.7664
	15.6	0.7687
Λ CDM	—	0.8123

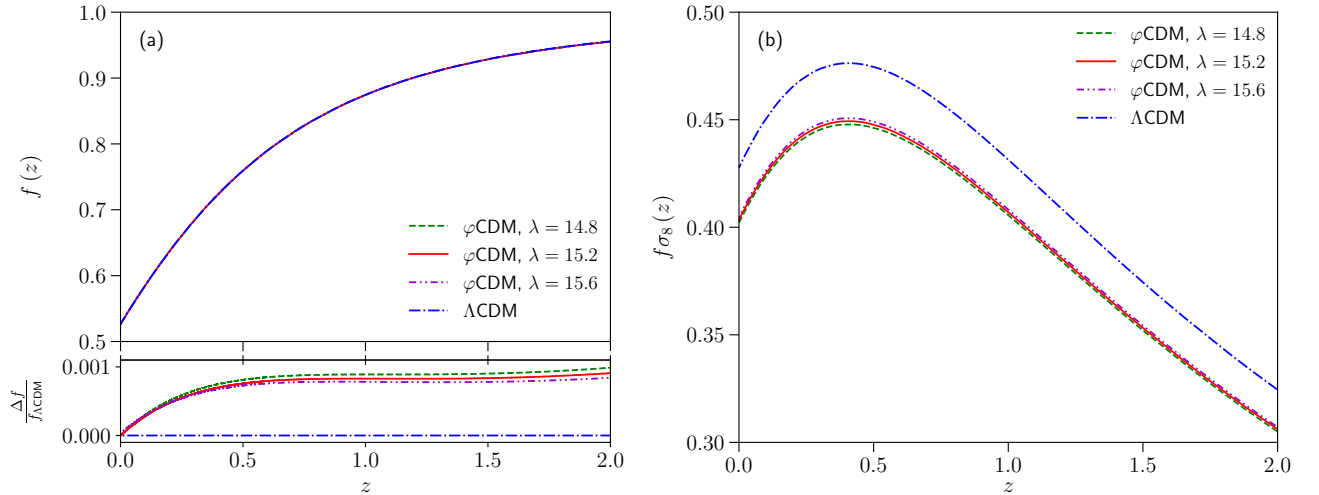


Figure 8: (a) Plot of **Upper Panel** : linear growth rate f and **Lower Panel** : fractional growth rate, $\frac{\Delta f}{f_{\Lambda\text{CDM}}} = \left(1 - \frac{f_{\phi\text{CDM}}}{f_{\Lambda\text{CDM}}}\right)$ relative to the Λ CDM model. (b) Plot of $f\sigma_8$ against redshift z . For all the plots, the dashed line represents ϕ CDM with $\lambda = 14.8$, solid line represents $\lambda = 15.2$ and dashed-dot-dot represents $\lambda = 15.6$ while the dashed-dot line is for Λ CDM.

The linear growth rate f is almost same for all the models at low redshift (Fig. (8a)). The little change in the growth rate, f due to change in λ is visible in the fractional change in growth rate, $\Delta f/f_{\Lambda\text{CDM}}$, relative to the Λ CDM model

(lower panel of Fig. (8a)). The difference in matter power spectrum is manifested in its amplitude σ_8 as given in Table (2) and hence in $f\sigma_8$ as in Fig. (8b). It is interesting to note that there is a substantial difference in $f\sigma_8$ for ϕ CDM and Λ CDM which is not there in the CMB temperature and matter power spectra. Thus, a low $f\sigma_8$ can be said to be the characteristic distinguishing feature of the present ϕ CDM model from the Λ CDM model. It must be noted that λ is chosen in such a way that is compatible with the age of the Universe which is around 13.797 ± 0.023 Giga years according to the recent *Planck* 2018 data [7].

4 Discussion

In the present work, we have introduced a scalar field model that will retain the virtues of the Λ CDM model without its shortcomings. We have investigated the perturbation in such a dynamical dark energy model that will alleviate the initial condition problem associated with the cosmological constant and attain an EoS parameter $w_\phi = -1$ at the present epoch. At early times the scalar field energy density tracks the dominant component of the background fluid and later on starts to roll sufficiently slowly to drive the accelerated expansion of the Universe. A scalar field with an exponential potential at early epoch and a constant potential at late time connected by Heaviside Θ functions (see Eqn. 6) appears to serve the purpose. That $w_\phi = -1$ for the present epoch is independent of the choice of the model parameters and the present dark energy density parameter, $\Omega_{\phi 0}$ is dependent on the height of the constant potential, V_0 .

We have worked out a detail perturbation analysis to differentiate the scalar field model (ϕ CDM) with the Λ CDM model. We have analysed the physical quantities that can be arrived at by solving the perturbation equations. The linearised scalar perturbations of the FLRW metric in synchronous gauge are studied using our modified CAMB. The growth of matter density contrast, δ_m is similar to the Λ CDM model and is smaller for the smaller value of λ . The linear growth rate f , which is the logarithmic derivative of δ_m with respect to a is same for both the models. The presence of the scalar field slightly decreases the matter content of the Universe during the evolutionary history. This decrease in matter content is manifested in the matter power spectrum and even more clearly in the evolution of the $f\sigma_8$. Thus, $f\sigma_8$ helps in breaking the degeneracy between the present ϕ CDM model and the standard Λ CDM. Another interesting result is that the decrease in the rate of clustering decreases the variance of the linear matter perturbation, σ_8 . As seen from Table (2), the σ_8 obtained here is more towards the side of the value obtained from the galaxy cluster counts using thermal Sunyaev-Zel'dovich (tSZ) signature [7, 88], $\sigma_8 = 0.77^{+0.04}_{-0.03}$ rather than the value obtained from *Planck* spectrum [7], $\sigma_8 = 0.811 \pm 0.006$. It must be mentioned here that as shown in [89, 90], quintessence-CDM model also prefer lower H_0 compared to the standard Λ CDM model. A detailed study of the parameter space is required to confirm if this model can solve the σ_8 tension and prefer a lower value of H_0 . Such an analysis is outside the scope of the present article and will be considered in a separate work. It has already been mentioned that the values of the background parameters ($\Omega_b h^2$, $\Omega_c h^2$, H_0 , A_s and n_s) are fixed to the mean values obtained by the *Planck* 2018 collaboration [7], for the fiducial spatially flat Λ CDM model. We have used them as an illustrative example in the absence of any parameter values obtained by constraining the present model with the observational data sets.

It can be said quite conclusively that this scalar field model resolves the initial condition problem, produces late-time acceleration with $w_\phi = -1$ as predicted by the recent data as well as decreases rms mass fluctuation σ_8 . This model is also successful in the context of the structure formation in the Universe. The model looks to be promising, but it has to be tested against observational datasets, and compared with Λ CDM and other competing models in connection with the evidence criteria.

References

- [1] A.G. Riess et al., *Observational evidence from supernovae for an accelerating universe and a cosmological constant*, *The Astronomical Journal* **116** (1998) 1009.
- [2] B.P. Schmidt et al., *The High-Z Supernova Search: Measuring Cosmic Deceleration and Global Curvature of the Universe Using Type Ia Supernovae*, *Astrophys. J.* **507** (1998) 46.
- [3] S. Perlmutter et al., *Measurements of Ω and Λ from 42 High-Redshift Supernovae*, *Astrophys. J.* **517** (1999) 565.
- [4] D.M. Scolnic et al., *The Complete Light-curve Sample of Spectroscopically Confirmed SNe Ia from Pan-STARRS1 and Cosmological Constraints from the Combined Pantheon Sample*, *Astrophys. J.* **859** (2018) 101.
- [5] D.J. Eisenstein, W. Hu and M. Tegmark, *Cosmic Complementarity: H_0 and Ω_m from Combining Cosmic Microwave Background Experiments and Redshift Surveys*, *Astrophys. J.* **504** (1998) L57.
- [6] Ade, P. A. R. and et al., *Planck 2015 results-XIII. Cosmological parameters*, *A&A* **594** (2016) A13.
- [7] PLANCK collaboration, *Planck 2018 results. VI. Cosmological parameters*, *Astron. Astrophys.* **641** (2020) A6.
- [8] M. Tanabashi et al., *Review of Particle Physics*, *Phys. Rev. D* **98** (2018) 030001.

- [9] B.A. Reid et al., *Cosmological constraints from the clustering of the Sloan Digital Sky Survey DR7 luminous red galaxies*, *Monthly Notices of the Royal Astronomical Society* **404** (2010) 60.
- [10] T.M.C. Abbott et al., *Cosmological Constraints from Multiple Probes in the Dark Energy Survey*, *Phys. Rev. Lett.* **122** (2019) 171301.
- [11] S. Alam et al., *The clustering of galaxies in the completed SDSS-III Baryon Oscillation Spectroscopic Survey: cosmological analysis of the DR12 galaxy sample*, *Monthly Notices of the Royal Astronomical Society* **470** (2017) 2617.
- [12] EBOSS collaboration, *The Completed SDSS-IV extended Baryon Oscillation Spectroscopic Survey: Cosmological Implications from two Decades of Spectroscopic Surveys at the Apache Point observatory*, 2007 .08991.
- [13] T. Padmanabhan, *Cosmological constant—the weight of the vacuum*, *Physics Reports* **380** (2003) 235.
- [14] E.J. Copeland, M. Sami and S. Tsujikawa, *Dynamics Of Dark Energy*, *International Journal of Modern Physics D* **15** (2006) 1753.
- [15] J.A. Frieman, M.S. Turner and D. Huterer, *Dark Energy and the Accelerating Universe*, *Annual Review of Astronomy and Astrophysics* **46** (2008) 385.
- [16] L. Amendola, K. Kainulainen, V. Marra and M. Quartin, *Large-scale inhomogeneities may improve the cosmic concordance of supernovae*, *Phys. Rev. Lett.* **105** (2010) 121302.
- [17] A. Mehrabi, *Growth of perturbations in dark energy parametrization scenarios*, *Phys. Rev. D* **97** (2018) 083522.
- [18] P.J.E. Peebles and B. Ratra, *Cosmology with a Time-Variable Cosmological “Constant”*, *Astrophysical Journal Letters* **325** (1988) L17.
- [19] B. Ratra and P.J.E. Peebles, *Cosmological consequences of a rolling homogeneous scalar field*, *Phys. Rev. D* **37** (1988) 3406.
- [20] J.A. Frieman, C.T. Hill, A. Stebbins and I. Waga, *Cosmology with ultralight pseudo Nambu-Goldstone bosons*, *Phys. Rev. Lett.* **75** (1995) 2077.
- [21] S.M. Carroll, *Quintessence and the rest of the world: Suppressing long-range interactions*, *Phys. Rev. Lett.* **81** (1998) 3067.
- [22] R.R. Caldwell, R. Dave and P.J. Steinhardt, *Cosmological imprint of an energy component with general equation of state*, *Phys. Rev. Lett.* **80** (1998) 1582.
- [23] V. Sahni and A. Starobinsky, *The case for a positive cosmological Λ -term*, *International Journal of Modern Physics D* **09** (2000) 373.
- [24] L.A. Ureña López and T. Matos, *New cosmological tracker solution for quintessence*, *Phys. Rev. D* **62** (2000) 081302.
- [25] S.M. Carroll, *The Cosmological Constant*, *Living Reviews in Relativity* **4** (2001) 1.
- [26] P.J.E. Peebles and B. Ratra, *The cosmological constant and dark energy*, *Rev. Mod. Phys.* **75** (2003) 559.
- [27] E.J. Copeland, M.R. Garousi, M. Sami and S. Tsujikawa, *What is needed of a tachyon if it is to be the dark energy?*, *Phys. Rev. D* **71** (2005) 043003.
- [28] J. Martin, *Quintessence: A mini-review*, *Modern Physics Letters A* **23** (2008) 1252.
- [29] J.-B. Durrive, J. Ooba, K. Ichiki and N. Sugiyama, *Updated observational constraints on quintessence dark energy models*, *Phys. Rev. D* **97** (2018) 043503.
- [30] M. Li, *A model of holographic dark energy*, *Physics Letters B* **603** (2004) 1.
- [31] D. Pavón and W. Zimdahl, *Holographic dark energy and present cosmic acceleration*, *AIP Conference Proceedings* **841** (2006) 356.
- [32] W. Zimdahl and D. Pavón, *Interacting holographic dark energy*, *Classical and Quantum Gravity* **24** (2007) 5461.
- [33] A. Kamenshchik, U. Moschella and V. Pasquier, *An alternative to quintessence*, *Physics Letters B* **511** (2001) 265.
- [34] N. Bilić, G.B. Tupper and R.D. Viollier, *Unification of dark matter and dark energy: the inhomogeneous chaplygin gas*, *Physics Letters B* **535** (2002) 17.

- [35] M.C. Bento, O. Bertolami and A.A. Sen, *Generalized Chaplygin gas, accelerated expansion, and dark-energy-matter unification*, *Phys. Rev. D* **66** (2002) 043507.
- [36] T. Chiba, T. Okabe and M. Yamaguchi, *Kinetically driven quintessence*, *Phys. Rev. D* **62** (2000) 023511.
- [37] R. Caldwell, *A phantom menace? cosmological consequences of a dark energy component with super-negative equation of state*, *Physics Letters B* **545** (2002) 23.
- [38] S.M. Carroll, M. Hoffman and M. Trodden, *Can the dark energy equation-of-state parameter w be less than -1 ?*, *Phys. Rev. D* **68** (2003) 023509.
- [39] B. Feng, X. Wang and X. Zhang, *Dark energy constraints from the cosmic age and supernova*, *Physics Letters B* **607** (2005) 35.
- [40] Y.-F. Cai, H. Li, Y.-S. Piao and X. Zhang, *Cosmic duality in quintom universe*, *Physics Letters B* **646** (2007) 141.
- [41] V. Sahni, *The cosmological constant problem and quintessence*, *Classical and Quantum Gravity* **19** (2002) 3435.
- [42] S. Tsujikawa, *Quintessence: a review*, *Classical and Quantum Gravity* **30** (2013) 214003.
- [43] M. Sami and R. Myrzakulov, *Late-time cosmic acceleration: ABCD of dark energy and modified theories of gravity*, *International Journal of Modern Physics D* **25** (2016) 1630031.
- [44] P. Brax, *What makes the Universe accelerate? A review on what dark energy could be and how to test it*, *Reports on Progress in Physics* **81** (2017) 016902.
- [45] P.J. Steinhardt, *A Quintessential Introduction to Dark Energy*, *Philosophical Transactions: Mathematical, Physical and Engineering Sciences* **361** (2003) 2497.
- [46] H.E.S. Velten, R.F. vom Martens and W. Zimdahl, *Aspects of the cosmological “coincidence problem”*, *The European Physical Journal C* **74** (2014) 3160.
- [47] P.G. Ferreira and M. Joyce, *Structure formation with a self-tuning scalar field*, *Phys. Rev. Lett.* **79** (1997) 4740.
- [48] E.J. Copeland, A.R. Liddle and D. Wands, *Exponential potentials and cosmological scaling solutions*, *Phys. Rev. D* **57** (1998) 4686.
- [49] P.G. Ferreira and M. Joyce, *Cosmology with a primordial scaling field*, *Phys. Rev. D* **58** (1998) 023503.
- [50] C. Wetterich, *Cosmology and the fate of dilatation symmetry*, *Nuclear Physics B* **302** (1988) 668.
- [51] G. Efstathiou, *Constraining the equation of state of the Universe from distant Type Ia supernovae and cosmic microwave background anisotropies*, *Monthly Notices of the Royal Astronomical Society* **310** (1999) 842.
- [52] J.E. Kim, *Axion and almost massless quark as ingredients of quintessence*, *Journal of High Energy Physics* **1999** (1999) 022.
- [53] I. Zlatev, L. Wang and P.J. Steinhardt, *Quintessence, cosmic coincidence, and the cosmological constant*, *Phys. Rev. Lett.* **82** (1999) 896.
- [54] P.J. Steinhardt, L. Wang and I. Zlatev, *Cosmological tracking solutions*, *Phys. Rev. D* **59** (1999) 123504.
- [55] P. Brax and J. Martin, *Quintessence and supergravity*, *Physics Letters B* **468** (1999) 40.
- [56] P. Brax and J. Martin, *Robustness of quintessence*, *Phys. Rev. D* **61** (2000) 103502.
- [57] T. Barreiro, E.J. Copeland and N.J. Nunes, *Quintessence arising from exponential potentials*, *Phys. Rev. D* **61** (2000) 127301.
- [58] V. Sahni and L. Wang, *New cosmological model of quintessence and dark matter*, *Phys. Rev. D* **62** (2000) 103517.
- [59] A. Albrecht and C. Skordis, *Phenomenology of a realistic accelerating universe using only Planck-scale physics*, *Phys. Rev. Lett.* **84** (2000) 2076.
- [60] S. Dodelson, M. Kaplinghat and E. Stewart, *Solving the coincidence problem: Tracking oscillating energy*, *Phys. Rev. Lett.* **85** (2000) 5276.
- [61] L. Wang, R.R. Caldwell, J.P. Ostriker and P.J. Steinhardt, *Cosmic concordance and quintessence*, *Astrophys. J.* **530** (2000) 17.

- [62] A. Sen and S. Sethi, *Quintessence model with double exponential potential*, *Physics Letters B* **532** (2002) 159.
- [63] L. Amendola, M. Quartin, S. Tsujikawa and I. Waga, *Challenges for scaling cosmologies*, *Phys. Rev. D* **74** (2006) 023525.
- [64] K. Dimopoulos and C. Owen, *Quintessential inflation with α -attractors*, *Journal of Cosmology and Astroparticle Physics* **2017** (2017) 027.
- [65] S.S. Mishra, V. Sahni and Y. Shtanov, *Sourcing dark matter and dark energy from α -attractors*, *Journal of Cosmology and Astroparticle Physics* **2017** (2017) 045.
- [66] N. Roy, A.X. Gonzalez-Morales and L.A. Ureña López, *New general parametrization of quintessence fields and its observational constraints*, *Phys. Rev. D* **98** (2018) 063530.
- [67] Z. Zhai, M. Blanton, A. Slosar and J. Tinker, *An Evaluation of Cosmological Models from the Expansion and Growth of Structure Measurements*, *The Astrophysical Journal* **850** (2017) 183.
- [68] C.-G. Park and B. Ratra, *Observational Constraints on the Tilted Spatially Flat and the Untilted Nonflat Φ CDM Dynamical Dark Energy Inflation Models*, *The Astrophysical Journal* **868** (2018) 83.
- [69] J. Ooba, B. Ratra and N. Sugiyama, *Planck 2015 constraints on spatially-flat dynamical dark energy models*, *Astrophysics and Space Science* **364** (2019) 176.
- [70] C.-G. Park and B. Ratra, *Using SPT polarization, Planck 2015, and non-CMB data to constrain tilted spatially-flat and untilted nonflat Λ CDM, XCDM, and ϕ CDM dark energy inflation cosmologies*, *Phys. Rev. D* **101** (2020) 083508.
- [71] S. Bag, S.S. Mishra and V. Sahni, *New tracker models of dark energy*, *Journal of Cosmology and Astroparticle Physics* **2018** (2018) 009.
- [72] L.R. Abramo, R.C. Batista, L. Liberato and R. Rosenfeld, *Physical approximations for the nonlinear evolution of perturbations in inhomogeneous dark energy scenarios*, *Phys. Rev. D* **79** (2009) 023516.
- [73] A. Mehrabi, S. Basilakos and F. Pace, *How clustering dark energy affects matter perturbations*, *Monthly Notices of the Royal Astronomical Society* **452** (2015) 2930.
- [74] R. Batista and F. Pace, *Structure formation in inhomogeneous Early Dark Energy models*, *Journal of Cosmology and Astroparticle Physics* **2013** (2013) 044.
- [75] P. Brax, J. Martin and A. Riazuelo, *Exhaustive study of cosmic microwave background anisotropies in quintessential scenarios*, *Phys. Rev. D* **62** (2000) 103505.
- [76] A. Lewis, A. Challinor and A. Lasenby, *Efficient Computation of Cosmic Microwave Background Anisotropies in Closed Friedmann-Robertson-Walker Models*, *Astrophys. J.* **538** (2000) 473.
- [77] J. Väliviita, E. Majerotto and R. Maartens, *Large-scale instability in interacting dark energy and dark matter fluids*, *Journal of Cosmology and Astroparticle Physics* **2008** (2008) 020.
- [78] C.-P. Ma and E. Bertschinger, *Cosmological perturbation theory in the synchronous and conformal Newtonian gauges*, *Astrophys. J.* **455** (1995) 7.
- [79] H. Kodama and M. Sasaki, *Cosmological Perturbation Theory*, *Progress of Theoretical Physics Supplement* **78** (1984) 1.
- [80] V. Mukhanov, H. Feldman and R. Brandenberger, *Theory of cosmological perturbations*, *Physics Reports* **215** (1992) 203.
- [81] K.A. Malik, D. Wands and C. Ungarelli, *Large-scale curvature and entropy perturbations for multiple interacting fluids*, *Phys. Rev. D* **67** (2003) 063516.
- [82] J.A.R. Cembranos, A.L. Maroto and S.J. Núñez Jareño, *Cosmological perturbations in coherent oscillating scalar field models*, *Journal of High Energy Physics* **2016** (2016) 13.
- [83] J. Martin and D.J. Schwarz, *Influence of cosmological transitions on the evolution of density perturbations*, *Phys. Rev. D* **57** (1998) 3302.
- [84] W. Hu and N. Sugiyama, *Anisotropies in the Cosmic Microwave Background: an Analytic Approach*, *Astrophys. J.* **444** (1995) 489.

- [85] U. Seljak and M. Zaldarriaga, *A Line-of-Sight Integration Approach to Cosmic Microwave Background Anisotropies*, *Astrophys. J.* **469** (1996) 437.
- [86] S. Dodelson, *Modern Cosmology*, Academic Press, Amsterdam (2003).
- [87] W.J. Percival and M. White, *Testing cosmological structure formation using redshift-space distortions*, *Monthly Notices of the Royal Astronomical Society* **393** (2009) 297.
- [88] Ì. Zubeldia and A. Challinor, *Cosmological constraints from Planck galaxy clusters with CMB lensing mass bias calibration*, *Monthly Notices of the Royal Astronomical Society* **489** (2019) 401.
- [89] A. Banerjee, H. Cai, L. Heisenberg, E.O. Colgáin, M. Sheikh-Jabbari and T. Yang, *Hubble Sinks In The Low-Redshift Swampland*, **2006**. 00244.
- [90] E. Ó Colgáin and H. Yavartanoo, *Testing the Swampland: H_0 tension*, *Physics Letters B* **797** (2019) 134907.